

Investigation of the magnetic dipole field at the atomic scale in quasi-one-dimensional paramagnetic conductor $\text{Li}_{0.9}\text{Mo}_6\text{O}_{17}$

Guoqing Wu,^{1,3} Bing Wu,² and W. G. Clark³

¹*College of Physics Science and Technology, Yangzhou University, Yangzhou, Jiangsu 225002, China*

²*Department of Math and Computer Science, Fayetteville State University, Fayetteville, NC 28301, USA and*

³*Department of Physics and Astronomy, University of California, Los Angeles, California 90095, USA**

(Dated: December 3, 2014)

We report magnetic dipole field investigation at the atomic scale in a single crystal of quasi-one-dimensional (Q1D) paramagnetic conductor $\text{Li}_{0.9}\text{Mo}_6\text{O}_{17}$, using a paramagnetic electron model and ^7Li -NMR spectroscopy measurements with an externally applied magnetic field $B_0 = 9$ T. We find that the magnetic dipole field component ($B_{\parallel}^{\text{dip}}$) parallel to B_0 at the Li site from the Mo electrons has no lattice axial symmetry; it is small around the middle between the lattice c and a axes in the ac -plane with the minimum at the field orientation angle $\theta = +52.5^\circ$, while the $B_{\parallel}^{\text{dip}}$ maximum is at $\theta = +142.5^\circ$ when B_0 is applied perpendicular to b ($B_0 \perp b$), where $\theta = 0^\circ$ represents the direction of $B_0 \parallel c$. Further estimate indicates that $B_{\parallel}^{\text{dip}}$ has a maximum value of 0.35 G at $B_0 = 9$ T, and the Mo ions have a possible effective magnetic dipole moment $0.015 \mu_B$ per ion, which is significantly smaller than that of a spin 1/2 free electron. By minimizing potential magnetic contributions to the NMR spectra satellites with the NMR spectroscopy measurements at the direction where the value of the magnetic dipole field is the smallest, the behavior of the independent charge contributions is observed. This work demonstrates that the magnetic dipole field from the Mo electrons is the dominant source of the local magnetic fields at the Li site, and it suggests that the mysterious “metal-insulator” crossover at low temperatures is not a charge effect. The work also reveals valuable local field information for further NMR investigation which is suggested recently [Phys. Rev. B **85**, 235128 (2012)] to be key important to the understanding of many mysterious properties of this Q1D material of particular interest.

PACS numbers: 75.30.Cr, 75.20.-g, 75.20.En, 76.60.-k

I. INTRODUCTION

The quasi-one-dimensional (Q1D) paramagnetic conductor, $\text{Li}_{0.9}\text{Mo}_6\text{O}_{17}$, has been of particular interest because of its unusual properties. It is thought to exhibit transport properties associated with a Luttinger liquid¹⁻³ at high temperatures, and otherwise many of its properties have long been mysterious⁴⁻⁸. Among these is an unusual increase (an upturn) in resistivity^{4,9,10}, which shows a “metal-insulator” crossover at low temperatures (the crossover temperature $T_{\text{MI}} = 24$ K), for which a robust explanation remains elusive, while four completely different mechanisms were theoretically proposed^{11,12}: charge-density wave (CDW), spin-density wave (SDW), localization, and Luttinger liquid. It is also a superconductor (“insulator”-superconductor transition temperature $T_c = 2.2$ K), which is most recently^{6,10} found to be three-dimensional (3D). Thus it involves an electron dimensional crossover,^{13,14} and may also involve spin triplet Cooper pairs^{6,15}, with a triplet superconducting state as one of its potential electron ground states.

$\text{Li}_{0.9}\text{Mo}_6\text{O}_{17}$ has also been a subject of intensive experimental studies over the last three decades^{4,5}. Many different types of experiments has been performed: x-ray diffraction¹⁶, neutron scattering¹³, dc magnetic susceptibility¹⁷⁻¹⁹, resistivity^{10,17,20,21}, heat capacity²², thermal expansion¹⁴, thermal conductivity^{8,23}, Nernst signal²⁴, optical conductivity¹⁷, muons spectroscopy²⁵, scanning tunneling microscope (STM)³, and angle re-

solved photo-emission (ARPES)²⁶. But it faces tremendous challenges over these experiments for the physics understanding. For example, for the “metal-insulator” crossover at 24 K, x-ray diffraction and neutron scattering show no evidence of structure phase transition^{13,16}, dc susceptibility shows no signs of Curie-Weiss deviation in the electron magnetization¹⁷⁻¹⁹, and heat capacity indicates negligible associated heat anomaly²².

Because of these challenges and the limitations in many of these experimental techniques, other capable experimental techniques are highly valuable. For example, most recent theoretical studies in $\text{Li}_{0.9}\text{Mo}_6\text{O}_{17}$ have strongly suggested^{7,27} the significance of charge and spin fluctuations & correlation which are related to the local electric and magnetic fields arising from the Mo electrons and could be measured at the Mo or nearby atom site like the Li. However, none of above experimental techniques were able to probe them directly at the atomic scale. On the other hand, in terms of a Luttinger liquid (if this is the case), long-range Coulomb interactions among the conduction electrons are expected^{1,2,7} to be stronger than those in a traditional Fermi liquid. The interaction could induce electron polarizations and thus have a direct impact on the local electric and magnetic fields. Therefore, it is important to investigate the local electric and magnetic field from the Mo electrons. Moreover, the field reveals the sources of the charge and spin dynamics^{28,29} of the Mo electrons at the atomic scale.

Nuclear magnetic resonance (NMR) is a well-known

versatile local probe capable of directly measuring the local electric and magnetic field including the electron charge and spin dynamics at the atomic scale^{28,29}.

In this paper, we report local electric and magnetic field investigation, using a theoretical paramagnetic electron model and ⁷Li-NMR spectroscopy measurements on a single crystal of Li_{0.9}Mo₆O₁₇, with an externally applied magnetic field $B_0 = 9$ T. Since we expect the magnetic dipole field from the paramagnetic Mo electrons to be one of the major local field sources (at least one of them) at the Li site according to the NMR theory^{28,29}, the magnetic dipole field is the focus in this investigation.

In fact, magnetic dipole field that originated from the magnetic dipole moments of the electron spins, including the unpaired spins of the paramagnetic conduction electrons, are of particular interest in various aspects of NMR, including NMR spectroscopy, Knight shift, spin-lattice relaxation, and spin-echo decay, especially when the dipolar hyperfine couplings to the electron spins are significant, or when the time scale of their fluctuations matches that of the dynamics for the spin-lattice relaxation or spin-echo decay rates in the materials^{28–30}. For example, a NMR spectrum could be inhomogeneously broadened and a Knight shift could have a significant value, due to the contribution of the magnetic dipole fields from the electron spins^{28–31}. Similar effect could also be generated by other local field sources at a nucleus when they are not negligible^{32–34}. Unlike other local field sources, magnetic dipole field is always associated with the size & orientation of the magnetic dipole moments, and depends on the dipolar hyperfine coupling between the nucleus and the electron spins at the atomic scale, which can be estimated from the structure of the crystal lattice theoretically and can also be measured by the NMR techniques experimentally.

Our main results are that the magnetic dipole field component ($B_{\parallel}^{\text{dip}}$) parallel to B_0 from the Mo electrons at the Li site is found to have no lattice axial symmetry; it is small around the middle between the lattice c and a axes in the ac -plane, $\sim 7.5^\circ$ closer to the a -axis for the central minimum which is at $\theta = +52.5^\circ$, and the maximum is at $\theta = +142.5^\circ$ when B_0 is applied perpendicular to b ($B_0 \perp b$) (note, θ is one of the orientation angles of B_0 , and $\theta = 0^\circ$ represents the direction of $B_0 \parallel c$). Our further estimate indicates that the maximum value of $B_{\parallel}^{\text{dip}}$ at the Li site is ~ 0.35 G when $B_0 = 9$ T $\perp b$, and the Mo ions have a possible effective magnetic dipole moment (μ_{eff}) of $0.015 \mu_B$, which is significantly smaller than that of a spin $S = 1/2$ free electron. By separating the charge contribution from a mixture of major magnetic contributions to the NMR spectra satellites with the NMR spectroscopy measurements at the direction where the value of the magnetic dipole field is the smallest (i.e., the magnetic contribution is minimized), the behavior of the independent charge contributions is observed.

This work demonstrates that the magnetic dipole field from the Mo electrons is the dominant source of the local

magnetic fields at the Li site, and suggests that the mysterious “metal-insulator” crossover at low temperatures is not a charge effect. The work also reveals valuable local electric and magnetic field information for further NMR investigation which is strongly suggested²⁷ recently to be key important to the understanding of many mysterious properties^{4,15,17} of this Q1D material.

The rest of the paper is organized as follows. First, Section II presents the calculation of the magnetic dipole field at the atomic scale in paramagnetic electron systems, which is described in a general form so that the method can be used for applications in other electron systems, and the field in the Q1D paramagnetic conductor Li_{0.9}Mo₆O₁₇ is calculated when a single crystal sample is exposed to an externally applied magnetic field B_0 . Second, Section III has the experimental result of the ⁷Li-NMR spectra corresponding to the result of the theoretical calculations obtained in Section II. Third, Section IV presents discussions regarding the electron model used in the study and related physics quantities. Finally, the conclusions are stated in Section V.

II. CALCULATION OF THE MAGNETIC DIPOLE FIELD AT THE ATOMIC SCALE

As illustrated in Fig. 1 (a), a magnetic dipole moment $\vec{\mu}_j$ from the electrons of an atom at the site M (electron moment site j) in the crystal lattice can produce a magnetic dipole field (\vec{B}_{ij}) at a nearby atom site P (field observation site i). The value of \vec{B}_{ij} is given by³⁵

$$\vec{B}_{ij} = \frac{\mu_0}{4\pi} \left[\frac{3 \vec{r}_{ij}(\vec{\mu}_j \cdot \vec{r}_{ij})}{r_{ij}^5} - \frac{\vec{\mu}_j}{r_{ij}^3} \right], \quad (1)$$

where \vec{r}_{ij} is the displacement vector from j to i ($M \rightarrow P$), and μ_0 is the permeability constant.

The total dipolar field (\vec{B}) at the observation site P is the summation of the field from the moments at all the moment sites j ,

$$\vec{B} \equiv \langle \vec{B}_i \rangle = \sum_j \langle \vec{B}_{ij} \rangle, \quad (2)$$

$$= \frac{\mu_0}{4\pi} \sum_j \left\langle \left[\frac{3 \vec{r}_{ij}(\vec{\mu}_j \cdot \vec{r}_{ij})}{r_{ij}^5} - \frac{\vec{\mu}_j}{r_{ij}^3} \right] \right\rangle, \quad (3)$$

$$= \frac{\mu_0}{4\pi} \sum_j \left[\frac{3 \vec{r}_{ij}(\langle \vec{\mu}_j \rangle \cdot \vec{r}_{ij})}{r_{ij}^5} - \frac{\langle \vec{\mu}_j \rangle}{r_{ij}^3} \right]. \quad (4)$$

The magnetization \vec{M} due to the electron moments is

$$\vec{M} = \sum_j \langle \vec{\mu}_j \rangle / V, \quad (5)$$

where V is the sample volume.

For paramagnetic electrons, \vec{M} essentially has a very accurate linear dependence³⁶ on the externally applied

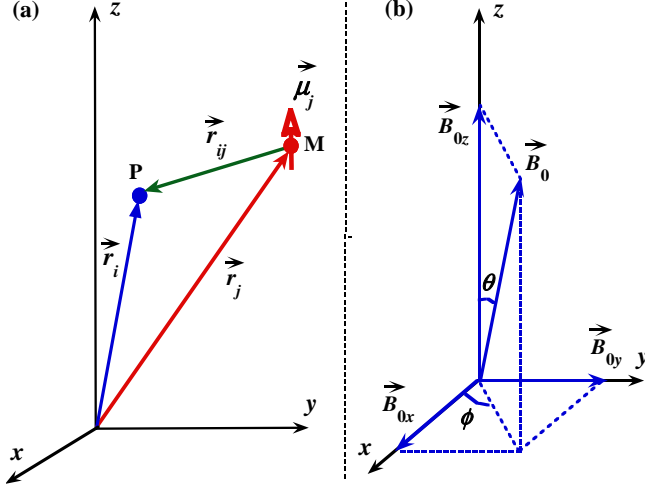


FIG. 1: (color online) (a) Cartesian coordinate system, where an electron magnetic dipole moment $\vec{\mu}_j$ is at the atom site M near the field observation site P in the crystal lattice. (b) The orientation of the externally applied magnetic field, \vec{B}_0 .

magnetic field \vec{B}_0 , i.e.,

$$\vec{M} = \chi \vec{H}_0, \text{ and } \vec{H}_0 = \vec{B}_0 / \mu_0, \quad (6)$$

where \vec{H}_0 is the intensity of the applied magnetic field, and χ is the sample paramagnetic susceptibility (isotropic), which can be a T -dependent variable [the deviation from their linear relation in Eq. (6) is in the order of $\sim \chi^2 \vec{H}_0$, which is negligible as $\chi < \sim 10^{-3}$ ($\text{cm}^3/\text{mol.ion}$) for most known materials]. If magnetic anisotropy is considered, then $M_{i'} = \chi_{i'j'} H_{0j'}$, where $\chi_{i'j'}$ is the tensor element of the susceptibility ($\chi_{i'j'} = \partial M_{i'} / \partial H_{0j'}$) and $i', j' = x, y, z$.

Thus considering Eqs. (1)-(6), we have

$$\vec{B} = \frac{\mu_0}{4\pi} \chi V \sum_{j=-N}^{+N} \left[\frac{3\vec{r}_{ij}(\vec{B}_0 \cdot \vec{r}_{ij})}{r_{ij}^5} - \frac{\vec{B}_0}{r_{ij}^3} \right], \quad (7)$$

where N in the index j is the number of sites for the electron moments. Equation (7) gives the x , y and z dipolar field components at the observation site i as

$$B_x = \frac{\mu_0}{4\pi} \chi V \sum_{j=-N}^{+N} \left[\frac{3x_{ij}(B_{0x}x_{ij} + B_{0y}y_{ij} + B_{0z}z_{ij})}{r_{ij}^5} - \frac{B_{0x}}{r_{ij}^3} \right], \quad (8)$$

$$B_y = \frac{\mu_0}{4\pi} \chi V \sum_{j=-N}^{+N} \left[\frac{3y_{ij}(B_{0x}x_{ij} + B_{0y}y_{ij} + B_{0z}z_{ij})}{r_{ij}^5} - \frac{B_{0y}}{r_{ij}^3} \right], \quad (9)$$

$$B_z = \frac{\mu_0}{4\pi} \chi V \sum_{j=-N}^{+N} \left[\frac{3z_{ij}(B_{0x}x_{ij} + B_{0y}y_{ij} + B_{0z}z_{ij})}{r_{ij}^5} - \frac{B_{0z}}{r_{ij}^3} \right]. \quad (10)$$

Figure 1 (b) shows the orientation of the applied magnetic field \vec{B}_0 , which can be expressed as $\vec{B}_0 = B_{0x}\hat{i} + B_{0y}\hat{j} + B_{0z}\hat{k} = B_0(\sin\theta\cos\phi\hat{i} + \sin\theta\sin\phi\hat{j} + \cos\theta\hat{k})$, where θ and ϕ are the standard spherical angles in the Cartesian system.³⁷

Thus the dipolar field components B_x , B_y , and B_z along the x , y , and z directions, respectively, can be calculated with Eqs. (8)-(10) by considering the coordinates of all the electron moment sites (atom sites M) that are included (as many as possible).

When the values of \vec{B} obeys $|\vec{B}| \ll B_0$, the contribution of \vec{B} to an NMR spectrum and Knight shift comes only from the component of $\vec{B} \parallel \vec{B}_0$ ($B_{\parallel}^{\text{dip}}$), which is also the case in our experimental observations with an applied magnetic $B_0 = 9$ T.

The calculation using Eqs. (8)-(10) requires Cartesian coordinates, thus for coordinates given in the lattice abc -system a transform matrix (M_{tran}) is needed. This can

be done by a fixed set-up of the Cartesian x , y , and z axes versus the a , b , and c axes of the crystal lattice in the lattice coordinate system that can always be made, where xz -plane is chosen to be placed in the ac -plane and the z -axis is along the c -axis, as illustrated in Fig. 2, from which we have

$$\vec{e}_a = (\sin\beta, 0, \cos\beta), \quad (11)$$

$$\vec{e}_b = (\sin\varphi\sin\delta, \cos\varphi, \sin\varphi\cos\delta), \quad (12)$$

$$\vec{e}_c = (0, 0, 1), \quad (13)$$

where \vec{e}_a , \vec{e}_b , and \vec{e}_c are the Cartesian expression for the unit vectors of the a , b , and c axes of the crystal lattice in the lattice coordinate system, respectively, and

$$\vec{e}_a \cdot \vec{e}_b = \cos\gamma, \text{ and } \vec{e}_b \cdot \vec{e}_c = \cos\alpha. \quad (14)$$

This gives

$$\sin\varphi\sin\delta = \frac{\cos\gamma - \cos\alpha\cos\beta}{\sin\beta}, \quad (15)$$

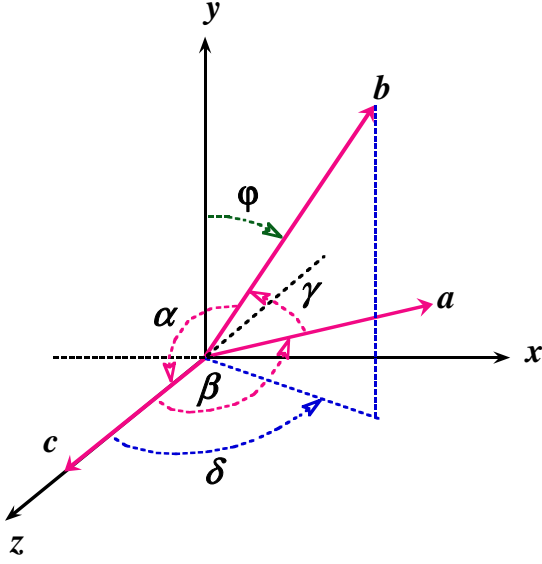


FIG. 2: (color online) A fixed set-up of the Cartesian x , y , and z axes relative to the a , b , and c axes of the crystal lattice in the lattice coordinate system that can always be made, where the xz -plane is in the ac -plane and the z -axis is along the c -axis.

$$\sin\varphi\cos\delta = \cos\alpha, \quad (16)$$

$$\cos\varphi = \sqrt{\sin^2\alpha - \left(\frac{\cos\gamma - \cos\alpha\cos\beta}{\sin\beta}\right)^2}. \quad (17)$$

By considering Eqs. (11) - (17), we have

$$\begin{pmatrix} \vec{e}_a \\ \vec{e}_b \\ \vec{e}_c \end{pmatrix} = \begin{pmatrix} \sin\beta & 0 & \cos\beta \\ \frac{\cos\gamma - \cos\alpha\cos\beta}{\sin\beta} & \sqrt{\sin^2\alpha - \left(\frac{\cos\gamma - \cos\alpha\cos\beta}{\sin\beta}\right)^2} & \cos\alpha \\ 0 & 0 & 1 \end{pmatrix} \begin{pmatrix} \vec{e}_x \\ \vec{e}_y \\ \vec{e}_z \end{pmatrix}, \quad (18)$$

or

$$(x, y, z) \begin{pmatrix} \vec{e}_x \\ \vec{e}_y \\ \vec{e}_z \end{pmatrix} = \begin{pmatrix} \sin\beta & \frac{\cos\gamma - \cos\alpha\cos\beta}{\sin\beta} & 0 \\ 0 & \sqrt{\sin^2\alpha - \left(\frac{\cos\gamma - \cos\alpha\cos\beta}{\sin\beta}\right)^2} & 0 \\ \cos\beta & \cos\alpha & 1 \end{pmatrix} (x'_a, y'_b, z'_c) \begin{pmatrix} \vec{e}_a \\ \vec{e}_b \\ \vec{e}_c \end{pmatrix}, \quad (19)$$

where α , β , and γ are the lattice constants (including the values of a , b and c), x'_a , y'_b , and z'_c are the atom coordinates in the lattice abc -coordinate system, and \vec{e}_x , \vec{e}_y , and \vec{e}_z are the unit vectors of the Cartesian x , y , and z axes, respectively. Thus with Eq. (18) or (19) the coordinates between the lattice and Cartesian coordinate systems are easily transformable.

In the following, the dipolar field in the Q1D paramagnetic conductor $\text{Li}_{0.9}\text{Mo}_6\text{O}_{17}$ is calculated.

The crystal lattice^{13,16} of $\text{Li}_{0.9}\text{Mo}_6\text{O}_{17}$ has a monoclinic space group $P2_1/m$, which has four equivalent sites in total for each site due to the symmetry of its 2-fold screw axis (b is the default axis for the rotation). The space group also has an existence of a mirror plane, which is $\perp b$. The four equivalent sites are

$$\begin{aligned} &(x', y', z') \\ &(-x', 1/2 + y', -z') \\ &(-x', -y', -z') \\ &(x', 1/2 - y', z'), \end{aligned}$$

i.e., each of which has the rest of three other equivalent sites to it. Here x' , y' , and z' are the fractional coordinates in the lattice abc -system, and their relation with x'_a , y'_b , and z'_c in Eq. (19) is, $x'_a = ax'$, $y'_b = by'$, and $z'_c = cz'$, respectively.

Figure 3 shows the crystal structure^{13,38} of $\text{Li}_{0.9}\text{Mo}_6\text{O}_{17}$. In each unit cell, there are six independent Mo sites, Mo1, Mo2, ..., Mo6, where the paramagnetic conduction electrons (with magnetic

TABLE I: The fractional coordinates for the positions of the independent Mo and Li sites in the unit cell with the lattice constants in the lattice coordinate system (value at 300 K). [Ref. 16]

atom sites	x'	y'	z'
Mo(1)	-0.00613	0.25	0.23356
Mo(2)	0.14436	0.75	0.41840
Mo(3)	0.31105	0.25	0.56755
Mo(4)	0.16635	0.25	-0.07938
Mo(5)	0.31980	0.75	0.09404
Mo(6)	0.49299	0.25	0.19604
Li	0.40240	0.75	0.40904

$a = 12.762$ (Å)	space group $P2_1/m$ (monoclinic)
$b = 5.523$ (Å)	
$c = 9.499$ (Å)	
$\alpha = 90^\circ$	
$\beta = 90.61^\circ$	
$\gamma = 90^\circ$	unit cell volume $v = 669.5$ (Å) ³

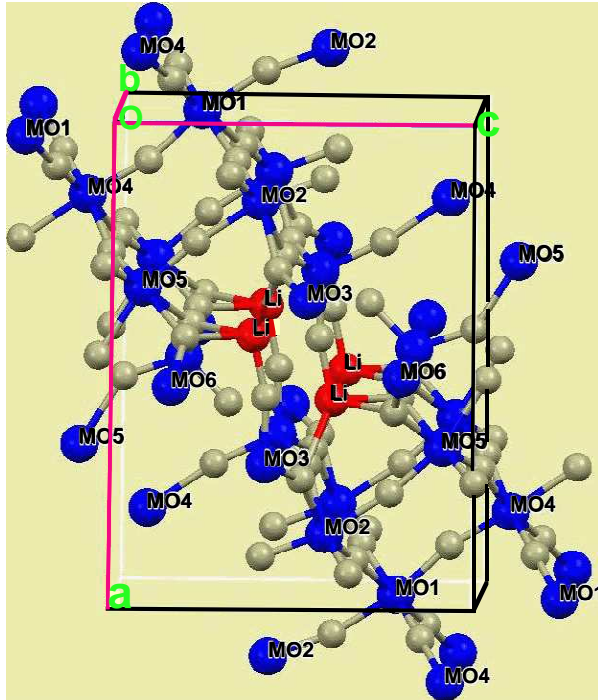


FIG. 3: (color online) The crystal structure of $\text{Li}_{0.9}\text{Mo}_6\text{O}_{17}$ obtained from the neutron scattering data.^{13,38} All the Mo (blue color) and Li (red color) atoms in a unit cell are labeled, while the unlabeled ones (grey color) are the O (oxygen) atoms. The lattice a , b and c axes are specified with the lines in pink color.

dipole moments) are from, while the number of independent sites for the Li (field observation site here) is only one. However, each site of them has three other sites, all of which are structurally equivalent to each other, as described above. Thus, in total there are 24 (6×4) Mo

sites and 4 Li sites (again, all the Li sites are equivalent in the crystal structure) in each unit cell. Apparently, all the 24 Mo sites (each has a magnetic dipole moment) contribute to the dipolar fields at the Li sites, while the fields at the Li sites are the same. Even so, there will still be a large number of terms in the dipolar field calculations.

Table I shows the fractional coordinates x' , y' , and z' for the positions of the independent Mo and Li sites in a unit cell (with the lattice constants) in the lattice coordinate system that are needed for the calculations.

With the matrix transform using Eq. (19), these fractional coordinates x' , y' , and z' in a unit cell (for convenience, let's number it as $N' = 0$) can be transformed into the Cartesian coordinates correspondingly. The same way needs to be applied to each neighboring unit cell ($N' = \pm 1, \pm 2, \pm 3, \dots$) along $\pm \vec{e}_x$, $\pm \vec{e}_y$ and $\pm \vec{e}_z$, correspondingly, with the values of x , y , and z to be used in Eqs. (8) - (10).

Figure 4 exhibits the calculated result of the magnetic dipole field components at the Li site due to the paramagnetic Mo electron moments in $\text{Li}_{0.9}\text{Mo}_6\text{O}_{17}$, plotted as H_x/M , H_y/M , and H_z/M versus θ and ϕ (in arbitrary unit which leaves out the constant $\mu_0/4\pi$ in front) along the x , y , and z directions, respectively, where M is the magnitude of the magnetization, and H_x , H_y , and H_z are the x , y , and z components of the calculated magnetic dipole field intensity, respectively [Eqs. (6) - (10)].

The calculation involves $N' = 10$, i.e., $(2N' + 1) = 21$ unit cells along each axial (x , y and z) direction (within a radius of ~ 130 Å). We also checked some calculations with $N' = 50$ and 100, and the results are essentially the same. Noticeably, the values of H_x/M , H_y/M , and H_z/M are completely determined by the lattice structure and the direction of B_0 , while independent of the magnetic susceptibility χ and the magnitude of B_0 .

As we can see from Fig. 4, each component including

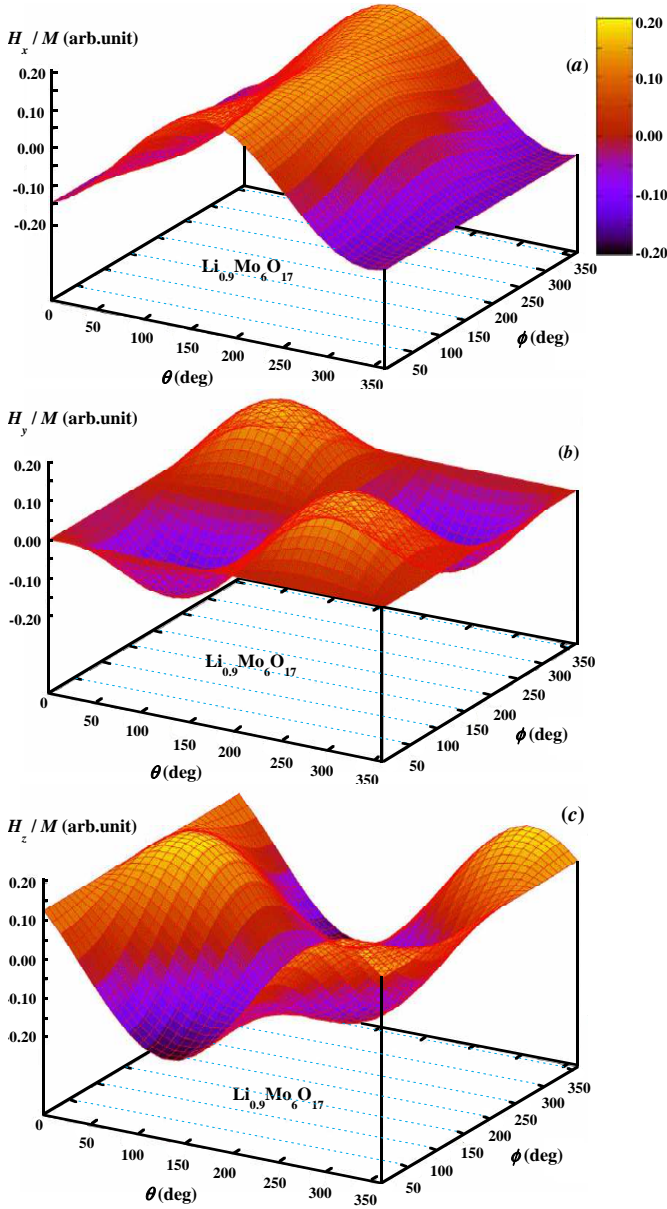


FIG. 4: (color online) Calculated magnetic dipole field components at the Li site in $\text{Li}_{0.9}\text{Mo}_6\text{O}_{17}$, as a function of the \vec{B}_0 orientation angles θ and ϕ in space, plotted as: (a) H_x/M , (b) H_y/M , and (c) H_z/M versus θ and ϕ along the x , y and z axes, respectively. Here M is the magnitude of the magnetization due to the electron paramagnetic moment.

its minimum and maximum values has a rather strong angular dependence (i.e., the direction of \vec{B}_0). For example, for $B_0 \perp b$ (i.e., $\phi = 0^\circ$), the minimum for H_x , H_y , and H_z is at $\theta = +340^\circ$, $+30^\circ$, and $+130^\circ$ (angle θ_{\min}), respectively, while the corresponding maximum is at $\theta = +160^\circ$, $+210^\circ$, and $+310^\circ$ (angle θ_{\max}), respectively. Thus, the angle difference between the maximum and minimum for each component always has $\theta = |\pm 180^\circ|$ (for $\phi = 0^\circ$). Moreover, we also have the absolute values for the minimum and maximum for each compo-

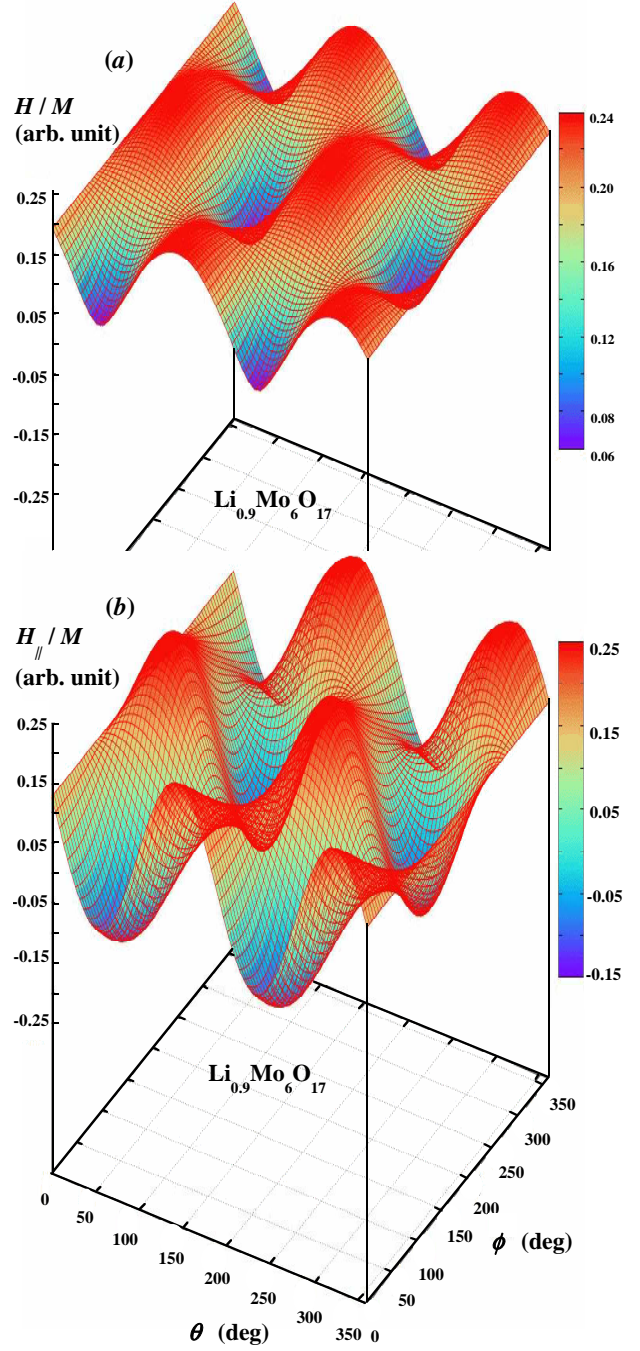


FIG. 5: (color online) Calculated (a) magnetic dipole field magnitude and (b) magnetic dipole field component parallel to \vec{B}_0 at the Li site in $\text{Li}_{0.9}\text{Mo}_6\text{O}_{17}$, as a function of (θ, ϕ) for the direction of \vec{B}_0 in space, plotted as H/M , and (b) H_{\parallel}/M , respectively.

nent to be the same, i.e., $|\min(H_k)| = -|\max(H_k)|$ (here $k = x, y$, and z), and the minimum (maximum) for H_y is the lowest among them (i.e., $H_y \ll H_x$ and $H_y \ll H_z$) when $\phi = 0^\circ$. These are understandable because the paramagnetic electron moment tends to align along B_0 , and B_0 is perpendicular to the y (b) axis (H_y compo-

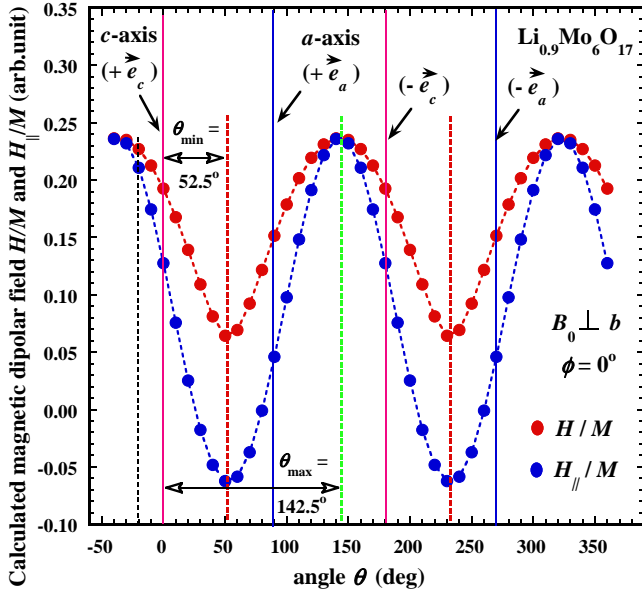


FIG. 6: (color online) Calculated magnetic dipole field magnitude (H/M) (red dots/curve) and magnetic dipole field component parallel to \vec{B}_0 (H_{\parallel}/M) (blue dots/curve) at the Li site in $\text{Li}_{0.9}\text{Mo}_6\text{O}_{17}$, as a function of angle θ for the direction of \vec{B}_0 when $\phi = 0$ ($B_0 \perp b$). The thin solid lines are labeled with arrows for the positions of the lattice a and c axes, and the thin dashed line (black color) at the angle $\theta = -20^\circ$ indicates an angle that some of our experimental observations are at. The rest of the thick dashed lines indicate the angles at which the values of H/M and H_{\parallel}/M in minimum and maximum are.

ment), i.e. B_0 is in the xz -plane which has the H_x and H_z components, when $\phi = 0^\circ$.

On the other hand, that we have $|\min(H_k)| = -|\max(H_k)|$ here instead of $|\min(H_k)| = -|\max(H_k)|/2$ or $|\min(H_k)| = -2|\max(H_k)|$ indicates that there is no axial symmetry for the magnetic dipole field components from the Mo-electrons observing at the Li site in $\text{Li}_{0.9}\text{Mo}_6\text{O}_{17}$, as an axial symmetry would expect a $\pm(3\cos^2\theta - 1)$ relation for a dipolar field as a function of θ , which also requires the minimum of H_k to be at $+54.7^\circ$ ($\pm 180^\circ$), an angle called the “magic angle” (θ_{magic}),^{29,35} i.e., $\theta_{\min} = \theta_{\text{magic}} \equiv +54.7^\circ \pm 180^\circ$, corresponding to the angle θ that satisfies $3\cos^2\theta - 1 = 0$.

Figure 5 shows the result of the calculated magnetic dipole field component parallel to the externally applied magnetic field B_0 [Fig. 5(b)], as compared with the magnitude of the magnetic dipole field [Fig. 5(a)] at the Li site, due to the paramagnetic Mo electron moments in $\text{Li}_{0.9}\text{Mo}_6\text{O}_{17}$. They are obtained based on the result shown in Fig. 4, plotted as H_{\parallel}/M and H/M versus θ and ϕ , respectively, with mathematical expressions for them as, $H_{\parallel} = \vec{H} \cdot \vec{B}_0 = H_x \sin\theta \cos\phi + H_y \sin\theta \sin\phi + H_z \cos\theta$, and $H = \sqrt{H_x^2 + H_y^2 + H_z^2}$.

Figure 5 indicates that H_{\parallel} and H have similar strong angular dependence with (θ, ϕ) to the axial dipolar field

components H_x , H_y and H_z , while their periods with both of the θ and ϕ dependence are essentially half of those for the axial dipolar field components, as we would expect since the values of the H_y component here are generally a lot smaller than other components [Fig. (4)] as a major factor here.

One aspect for the importance of the H_{\parallel} component is that H_{\parallel} is the only component (i.e., $B_{\parallel}^{\text{dip}}$) in terms of the magnetic dipole field \vec{H} that contributes to the Knight shift of a NMR spectrum, as mentioned earlier using $B_{\parallel}^{\text{dip}}$ ($\vec{B} \parallel \vec{B}_0$), where $B = \mu_0 H$ ($B_{\parallel}^{\text{dip}} = \mu_0 H_{\parallel}$), under the high field limit ($B \ll B_0$).

Figure 6 shows the detailed values of H_{\parallel} and H for $\phi = 0$ ($B \perp b$) as a function of θ , which is exactly the case when the sample is set to rotate around the b -axis in the applied magnetic field B_0 as we had in our NMR experiments,³⁹ while during the sample rotation \vec{B}_0 is kept in the xz -plane (also the ac -plane here for $\text{Li}_{0.9}\text{Mo}_6\text{O}_{17}$).

Interestingly, Fig. 6 indicates that 1) H_{\parallel} has the same maximum value as H [i.e., $\max(H_{\parallel}/M) = \max(H/M) \sim +0.24$ (arb.unit)], whereas their minimum values are very different, 2) the angles for their values in maximum are the same and the angles for their values in minimum are also the same. Their maximum and minimum values are at $\theta = \sim +142.5^\circ \pm 180^\circ$ (θ_{\max}) and $\theta = \sim +52.5^\circ \pm 180^\circ$ (θ_{\min}), respectively, and 3) a range of angles for the small values of H_{\parallel} are at the angles around the middle between the a and c axes in the ac -plane [i.e., at $\theta = \sim (50 \pm 30)^\circ$] (the minimum is 7.5° closer to the a -axis than to the c -axis). In order words, at the angles closer to the a -axis ($45^\circ < \theta \leq 90^\circ$), the value of H_{\parallel} is essentially negligible, and there is no axial symmetry (in terms of a dipolar field) for H_{\parallel} , either, observing from the Li site.

III. RESULT OF THE ^7Li -NMR EXPERIMENTAL OBSERVATIONS

Figure 7 shows the result of the measured ^7Li -NMR spectra of $\text{Li}_{0.9}\text{Mo}_6\text{O}_{17}$, with $B_0 = 9$ T applied $\perp b \sim$ along the lattice a -axis, $\phi = 0^\circ$ and $\theta = 90^\circ$, at two typical temperatures $T = 275$ K and 6 K, plotted as the spectrum absorption versus frequency shift (a shift from the NMR Larmor frequency $\nu_0 = \gamma_I B_0 = 148.95 \times 10^3$ kHz here, where $\gamma_I = 16.547$ MHz/T is the gyromagnetic ratio of the ^7Li nucleus). The details for the measurements will be published elsewhere³⁹.

For comparison, the spectra are normalized to be 1 in a standard way for the intensity of the central line and shifted on top of each other. Since ^7Li is a spin $I = 3/2$ nucleus, theoretically, each ^7Li -NMR spectrum is expected to have a central line plus two symmetric quadrupolar satellites due to the ^7Li nucleus spin quantum $m = +1/2 \leftrightarrow -1/2$ (central) and $\pm 3/2 \leftrightarrow \pm 1/2$ (satellites) transitions, respectively. This is exactly what we experimentally see here, verifying that all the Li sites

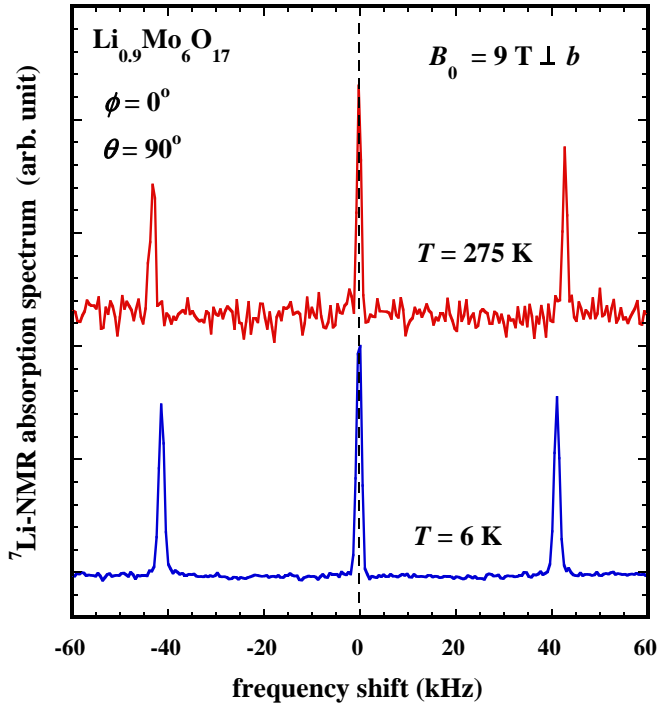


FIG. 7: (color online) Measured ${}^7\text{Li}$ -NMR spectra of $\text{Li}_{0.9}\text{Mo}_6\text{O}_{17}$, with $B_0 = 9 \text{ T} \perp b$ (i.e., $\phi = 0^\circ$) and \sim along the lattice a -axis (i.e., $\theta = 90^\circ$) at temperature $T = 275 \text{ K}$ (upper red curve) and 6 K (lower blue curve). For comparison, the spectra are normalized and shifted on top of each other as indicated by the dashed line at the center (black color). Note, that the satellite peaks are lightly closer to the central line at 6 K than at 275 K is caused³⁹ by a $\sim \pm 1^\circ$ angle change ($\Delta\theta$) due to the NMR sample probe thermal contraction upon cooling, with an extremely high sensitivity of the ${}^7\text{Li}$ -NMR quadrupole frequency at $B_0 \parallel a$.

are structurally equivalent with a high quality sample being used³⁹.

Figure 7 shows that the width of the ${}^7\text{Li}$ -NMR spectrum central line, more precisely, the full width half maximum (FWHM) of the central linewidth, has negligible change over a wide range of temperature from $T = 275 \text{ K}$ to 6 K , with a value of $\sim 0.6 \text{ kHz}$, including at the “metal-insulator” crossover temperature $T_{\text{MI}} = 24 \text{ K}$, i.e., there is no observable inhomogeneous magnetic broadening over a wide range of temperature (upon cooling from 275 K to 6 K), while during which range the sample magnetic susceptibility $\chi_{\text{DC}}(T)$ has a change of ~ 2 times. This spectrum data indicates that the distribution of the local magnetic field parallel to B_0 has no change.

Since the field distribution is proportional^{28,29} to the sample dc magnetic susceptibility $\chi_{\text{DC}}(T)$ and the strength of the dipolar coupling between the ${}^7\text{Li}$ nucleus and the Mo electrons H_{\parallel}/M ($B_{\parallel}^{\text{dip}}$), which is the major source of the local magnetic field at the ${}^7\text{Li}$ nucleus (see Sect. IV Discussion for details), this experimental spec-

trum data demonstrates that the value of H_{\parallel}/M ($B_{\parallel}^{\text{dip}}$) is very small for $B_0 \parallel a$ ($\phi = 0^\circ$ and $\theta = 90^\circ$) at the Li site, agreeing with the result of the theoretical calculations (Fig. 6).

This observation is further confirmed by our ${}^7\text{Li}$ -NMR spectra versus angle data,³⁹ for example, the correspondingly case at $\phi = 0^\circ$ and $\theta = -20^\circ$ or $+142.5^\circ$, where the value of $B_{\parallel}^{\text{dip}}$ is relatively large or has a maximum (near $B_0 \parallel c$), is very different (not shown here).

On the other hand, a NMR spectrum line can have a mixture of many different sources of local electric and/or magnetic field contributions (Sect. IV D). According to the NMR theory^{28,29}, the satellites and the central line of the ${}^7\text{Li}$ -NMR spectra have completely different origins: the central line is magnetic, due to the contribution of the nuclear spin interaction with the surrounding electron spins and other sources of the local magnetic fields, while the satellites are quadrupolar, coming from the contribution of the nuclear quadrupole moment interaction with the electric field gradient (EFG) due to the charges of the surrounding electrons (Mo electron charge contribution), i.e., the satellites are non-magnetic. Note, the quadrupolar interaction contribution (electric) to the central line is in the second order, thus having a negligible effect to the central line (non-electric). But its contribution to the satellites is in the first order, which is dominant (electric).

However, a satellite can be both electronically and magnetically broadened. Thus, in terms of judging the charge contributions by an NMR spectrum satellite, it is important to separate or minimize any potential magnetic contributions in any way possible. That is exactly why we have the ${}^7\text{Li}$ -NMR spectrum measurements at the direction \sim along the a -axis (Fig. 7), where the magnetic dipole field has \sim the smallest values (Fig. 6).

Therefore, from the fact that Fig. 7 also shows that the satellites of the ${}^7\text{Li}$ -NMR spectra including their FWHM width (the distribution of the EFG) have no changes, upon cooling in temperature, during which process the magnetic dipole field contributions to the satellites at $\theta = 90^\circ$ is minimized (close to zero), we can see that there is no appearance of any charge effect anomaly during the cooling process, thus suggesting that the “metal-insulator” crossover at $T_{\text{MI}} = 24 \text{ K}$ is not a charge effect.

IV. DISCUSSION

In this section, we have discussions regarding the paramagnetic electron model used in the above calculations, the Pauli spin susceptibility (χ_s) of the Mo electrons, the value of $B_{\parallel}^{\text{dip}}$ in Gauss (G) [at $B_0 = 9 \text{ T}$, for example], the major sources of the local magnetic fields at the Li site, and possible effective magnetic dipole moment (μ_{eff}) of the Mo electrons.

A. Paramagnetic electron model used in the calculation

In Sect. II, the magnetic dipole field in the quasi-one-dimensional (Q1D) paramagnetic conductor $\text{Li}_{0.9}\text{Mo}_6\text{O}_{17}$ is calculated when a single crystal sample is exposed to an externally applied magnetic field (B_0), using a paramagnetic electron model.

The method involves a summation of the magnetic dipole fields from the average of the individual magnetic dipole moments of the electron spins in the crystal lattice in component forms, each of which converges with the increase of the number (up to 100) of the unit cells to be included, within a spherical distance centering at the observation atom (or nucleus) site. It also involves a general matrix transform corresponding to a fixed set-up of the Cartesian x , y , and z axes relative to the a , b , and c axes of the crystal lattice in the lattice coordinate system that can always be made.

Here we would like to point out that, in the paramagnetic electron model used for the above calculation, possible differences of the electron moments among the six independent Mo sites in the structure are not considered. Instead, we use their average magnetic dipole moments as reflected by the magnetization M or magnetic susceptibility χ [Eqs. (5) - (6)]. We also neglect the individual electron interactions among the Mo electrons. Note, the interaction could polarize the electron dipole moments, which could also be reflected by the susceptibility data χ (see Sect. IV B).

Even so, it is still worthwhile to notice the possible difference in the electron moments and potential electron interactions, especially considering that some of the Mo electrons may not be equally conducting (or not conducting) according to their positions in the crystal lattice. In fact, along the a -axis in the crystal structure there are stacking layers (in the bc -plane) of Mo_4 octahedra separated by Mo_4 tetrahedra and the Li ions^{9,16}, and along the b -axis there is a double zig-zag Mo1-O-Mo4-O chain^{9,16,40}. Each chain involves only 2 (i.e., Mo1 and Mo4) out of 6 independent Mo sites (Mo1, Mo2,..., Mo6) that are believed^{20,40,41} to have the electrons being the most conducting (conduction electrons), above the mysterious metal-insulator cross-over temperature at $T_{\text{MI}} = 24 \text{ K}$ ^{4,17}. But below T_{MI} there is a gradual dimensional crossover¹³ and finally $\text{Li}_{0.9}\text{Mo}_6\text{O}_{17}$ becomes a 3D superconductor at $T \leq 2.2 \text{ K}$ upon cooling in temperature with $B_0 = 0$ or $0 < B_0 < H_{c2}$ (upper critical field)^{10,15}.

However, there is no clear evidence of anisotropy in the dc magnetic susceptibility (χ_{DC}) which could reflect the difference in the electron moments and spin polarizations in $\text{Li}_{0.9}\text{Mo}_6\text{O}_{17}$, as the difference between the axial values of χ_{DC} that Matsuda *et al.* showed¹⁹ is actually rather small, which is very different from the high anisotropy character^{10,41} in its electrical properties.

B. Pauli spin susceptibility (χ_s) of the Mo electrons

It is well-known that the Pauli spin (paramagnetic) susceptibility χ_s comes from the contributions of the conduction electron spin moments only,⁴² and the dc magnetic susceptibility (χ_{DC}) has a general expression as $\chi_{\text{DC}}(T) = \chi_{\text{dia}} + \chi_s(T) + \chi_{\text{orb}} + \chi_{\text{other}}(T)$, where χ_{dia} and χ_{orb} are T -independent diamagnetic susceptibility and orbital susceptibility, respectively, and $\chi_{\text{other}}(T)$ comes from other sources, including the localized electron moments, lattice imperfection and/or impurities which could be also part of a Curie/Curie-Weiss paramagnetic contribution term and become dominant at low T .

The dc magnetic susceptibility (χ_{DC}) measurements in $\text{Li}_{0.9}\text{Mo}_6\text{O}_{17}$ show that^{17,43}

$$\chi_{\text{DC}} = \frac{C}{T + \theta_D} + \chi_{01}, \quad (T < 100 \text{ K}), \quad (20)$$

$$\text{and } \chi_{\text{DC}} \approx (0.30 - 0.40) \times 10^{-4} \text{ (cm}^3/\text{mol.FU)}, \quad (100 \text{ K} \leq T \leq 300 \text{ K}), \quad (21)$$

i.e., it has a Curie-Weiss susceptibility term appears at low temperatures ($T < 100 \text{ K}$), where the Curie-Weiss constant $C = (7.8 \pm 0.2) \times 10^{-4} \text{ cm}^3\text{K/mol.FU}$ (note, $\text{FU} \equiv \text{formula unit}$), $\theta_D = (6.1 \pm 0.2) \text{ K}$, and $\chi_{01} = (0.181 \pm 0.005) \times 10^{-4} \text{ cm}^3/\text{mol.FU}$. In the high T regime ($T \geq 100 \text{ K}$), χ_{DC} has a value from $\sim 0.40 \times 10^{-4} \text{ cm}^3/\text{mol.FU}$ at 300 K to $\sim 0.30 \times 10^{-4} \text{ cm}^3/\text{mol.FU}$ at 100 K [Eq. (21)], i.e., it slowly decreases with a very weak T -dependence (close to linear here) upon cooling as expected for a quasi-1D conductor, where the T -dependence could have a contribution from the Pauli spin susceptibility $\chi_s(T)$ (note, χ_s has T -dependence for a 1D or 3D conductor)⁴⁴.

From the diamagnetism of the ions, we have $\chi_{\text{dia}} = -2.62 \times 10^{-4} \text{ cm}^3/\text{mol.FU}$, and according to the estimate¹⁹ by Matsuda *et al.*, $\chi_{\text{orb}} \approx 2.0 \times 10^{-4} \text{ cm}^3/\text{mol.FU}$. But it seems impractical to have further separations among the susceptibility data.

Most recent specific heat measurement¹⁸ resulted in $\chi_s(T)$ at $T \rightarrow 0 \text{ K}$ as, $\chi_s(0) = 3.0 \times 10^{-6}$, i.e., $0.50 \times 10^{-4} \text{ cm}^3/\text{mol.FU}$ (a factor with the molar density $\rho = 0.0595 \text{ mol/cm}^3$ for $\text{Li}_{0.9}\text{Mo}_6\text{O}_{17}$), using the measured Sommerfeld constant $\gamma_S = 1.6 \text{ mJ/mol.K}^2$ and the assumption of the Sommerfeld-Wilson ratio^{18,27} $R \equiv 4\pi^2 k_B^2 \chi_s(0) / [3(g\mu_B)^2 \gamma_S] = 2$, which applies for strongly correlated electrons and/or systems with repulsive interactions (here μ_B is the Bohr magneton, k_B is the Boltzmann constant and g is the Lande g -factor). Thus based on the measured values of $\chi_{\text{DC}}(T)$ [Eqs. (20)-(21)], we can also estimate the value of $\chi_s(T)$ at $T = 300 \text{ K}$, $\chi_s(300 \text{ K}) \approx 3.6 \times 10^{-6}$, i.e. $0.60 \times 10^{-4} \text{ cm}^3/\text{mol.FU}$.

Noticeably, χ_s is just slightly larger than the high temperature value of χ_{DC} . This is due to the cancellation of the orbital susceptibility χ_{orb} with the diamagnetic susceptibility χ_{dia} , both of which are $\sim (5 - 6)$ times larger than the high temperature value of χ_{DC} .

Now, with the value of $\chi_s(0)$ we can find the density of

state (DOS) $D(E_F)$ at the Fermi energy (E_F) level^{36,44},

$$D(E_F) = \chi_s(0)/\mu_B^2 \approx 1.5 \text{ (state/eV.FU)}, \quad (22)$$

$$\approx 0.25 \text{ (state/eV.ion)}.$$

This value is close to the result obtained from the specific heat measurements, which is $D(E_F) = 3\gamma_S N e / (\pi^2 k_B^2) \approx 0.68 \text{ (state/eV.ion)}$, where N is the number of ions per unit cell, and e is the electron charge⁴².

Correspondingly, the value of E_F (at $T \rightarrow 0$) is⁴⁴

$$E_F = d/[2D(E_F)] \approx 6.0 \text{ (eV)}, \quad (23)$$

where d is the dimension for the conduction electrons. Here we had $d = 3$ for $\text{Li}_{0.9}\text{Mo}_6\text{O}_{17}$ as it becomes a 3D conductor (superconductor) at $T \rightarrow 0$ K; both Eq. (22) and (23) are for 3D (not 1D) electrons. In comparison, this value of E_F is slightly smaller than that of the free Cu electrons which has a value⁴² of $E_F = 7.8 \text{ eV}$.

C. Value of $B_{||}^{\text{dip}}$ in Gauss (G) at $B_0 = 9 \text{ T}$

Considering the unit (arbitrary) of $H_{||}/M$ shown in Figs. 5 - 6 and the Eqs. (6) - (10), we can have a convenient expression for $B_{||}^{\text{dip}}$ as

$$B_{||}^{\text{dip}} = \frac{\mu_0}{4\pi} \chi B_0 \cdot (H_{||}/M). \quad (24)$$

Similar expressions can also be used for the dipolar field magnitude B and the values of the corresponding axial components B_x , B_y and B_z ($\vec{B} = \mu_0 \vec{H}$), where the unit of \vec{B} is in Gauss (G) or tesla (T) ($1 \text{ T} = 10^4 \text{ G}$).

For example, at $B_0 = 9 \text{ T}$ with its direction angles $\phi = 0^\circ$ and $\theta = 142.5^\circ$, using the value of $H_{||}/M = 0.24$ shown in Fig. 6 and the value of $\chi_s(300 \text{ K}) \approx 0.6 \times 10^{-4} \text{ cm}^3/\text{mol.FU}$, equation (24) gives $B_{||}^{\text{dip}} \approx 0.35 \text{ G}$. This is the maximum (anisotropic) magnetic dipole field at the Li site that comes from the Mo-electron paramagnetic spins (magnetic dipole moments) in $\text{Li}_{0.9}\text{Mo}_6\text{O}_{17}$.

D. Major sources of the local magnetic fields at the Li site

The Hamiltonian (H_I) of the system for the ^7Li -NMR in $\text{Li}_{0.9}\text{Mo}_6\text{O}_{17}$ can be expressed as²⁸

$$H_I = H_{IZ} + H_{II} + H_{Ie}^Q + H_{Ie}^{\text{dip}} + H_{Ie}^{\text{contact}} + H^{\text{demag}} + H^{\text{Lor}}, \quad (25)$$

where H_{IZ} is the Zeeman Hamiltonian of the ^7Li nucleus in B_0 , H_{II} is the ^7Li - ^7Li nuclear dipolar interaction Hamiltonian, H_{Ie}^Q is the Hamiltonian of the ^7Li nuclear quadrupole interaction with the surrounding charges of the Mo electrons, H_{Ie}^{dip} and H_{Ie}^{contact} are the anisotropic dipolar hyperfine coupling and isotropic contact hyperfine to the Mo electron spins, respectively, and the last

two terms, H^{dem} and H^{Lor} , are the bulk demagnetization and Lorentz contributions, respectively^{28,30}. Except for the first term H_{IZ} which is for the Zeeman splitting of the ^7Li nucleus's spin interaction with B_0 , all of these terms contribute to the local magnetic or electric field at the Li site, contribute to the ^7Li -NMR spectra and cause the NMR frequency shifts.

Noticeably, among these terms, only H_{Ie}^Q is non-magnetic^{28,29}; it has the first order (dominant) contribution to the local electric field (including the electric field distributions) at the ^7Li sites, which can be fully reflected by the ^7Li -NMR spectrum satellites.

Thus, by measuring the ^7Li -NMR spectra and observing any potential changes of the spectrum satellites at the direction where the magnetic contributions (from the total of all the rest of the magnetic terms) to the satellites are minimized or zero, we can tell the behavior of the charges of the Mo conduction electrons precisely at the atomic scale, which is one of the major significances of this study.

Because the ^7Li nucleus has a small atomic number $Z = 3$, it is expected²⁹ that its contact hyperfine couplings to the Mo electrons (H_{Ie}^{contact}) is negligible. Thus, the system Hamiltonian can be re-written as

$$H_I \approx H_{IZ} + H_{II} + H_{Ie}^Q + H_{Ie}^{\text{dip}} + H^{\text{dem}} + H^{\text{Lor}}. \quad (26)$$

The term H_{II} has a local magnetic field contribution (B_{II}) in the order of $^7\mu_I/r^3$, i.e., $B_{II} \sim ^7\mu_I/r^3$, where $^7\mu_I$ is the spin moment of the ^7Li nucleus, and r is the distance between neighboring ^7Li nuclei. Considering the value of $^7\mu_I = ^7\gamma_I \hbar I$ (\hbar is the Planck's constant) and the minimum value of $r = 3.939 \text{ \AA}$ as well as the positions of ^7Li in the crystal lattice, we have a rough estimate on B_{II} , which has an upper limit of $\sim 0.2 \text{ G}$.

Since B_{II} is independent of temperature and unrelated to the Mo electron spins, it has no contribution to any potential line broadening of the ^7Li -NMR spectra. Thus, our interest is in the last three terms, H_{Ie}^{dip} , H^{dem} , and H^{Lor} , which are the terms related to the Mo electron spin dynamics and the local magnetic field properties at the Li site (again the term H_{Ie}^Q contributes to the local electric field only).

In above Section IV C, we have estimated that at $B_0 = 9 \text{ T}$ along the lattice a -axis direction ($\theta = 90^\circ$), H_{Ie}^{dip} has a dipolar field contribution $B_{||}^{\text{dip}} \approx 0.35 \text{ G}$ at $T = 300 \text{ K}$. Now, we can estimate the magnetic field contributions of H^{demag} and H^{Lor} as³⁰, $B^{\text{demag}} = -4\pi \cdot D \cdot \chi_{\text{DC}}(T)/(N_A \cdot v_{\text{Mo}})$, and $B^{\text{Lor}} = +4\pi/3 \cdot \chi_{\text{DC}}(T)/(N_A \cdot v_{\text{Mo}})$, respectively, where $D \approx 0.45$ is the estimated demagnetization factor along the a -axis according to the sample size, N_A is the Avogadro's number, and $v_{\text{Mo}} = 669.5/24 \text{ \AA}^3$ is the unit cell volume per Mo ion (Table I). Thus, with the value of $\chi_{\text{DC}}(T) \approx 0.4 \times 10^{-4} \text{ cm}^3/\text{mol.FU}$ (at $T = 300 \text{ K}$) we have³⁰

$$B^{\text{demag}} + B^{\text{Lor}} = 4\pi \cdot \left(\frac{1}{3} - D\right) \cdot \frac{\chi_{\text{DC}}(T)}{N_A \cdot v_{\text{Mo}}}, \quad (27)$$

$$\approx -0.05 \text{ (G)}.$$

Therefore, the dipolar field of the Mo electron spins, i.e. the contribution of Hamiltonian H_{Ie}^{dip} (field $B_{||}^{\text{dip}}$), is the dominant source of the local magnetic fields including the field dynamics at the Li site ($B_{||}^{\text{dip}} > |B^{\text{demag}}|$ and/or B^{Lor} , and $B_{||}^{\text{dip}} > B_{II}$). B^{demag} and B^{Lor} together here contribute little to the total local magnetic field at the Li site due to the very small value of χ_{DC} of the material, as evidence by the measured ^7Li -NMR spectrum data (Fig. 7) (they have negligible impact on the spectra as the temperature varies).

Note that any interaction among the Mo electrons in the crystal lattice will affect the polarization of the Mo electron spins, thereby modifying the dipolar field at the Li site from the Mo ions.

E. Possible effective magnetic dipole moment (μ_{eff}) of the Mo electrons

There are important studies⁴⁵ regarding how to obtain the possible effective magnetic dipole moment (μ_{eff}) of the conduction electrons as described in Ref. [45]. Similar method was used recently in Ref. [46], which supposes that the value of μ_{eff} is proportional to the spin susceptibility χ_s (both μ_{eff} and χ_s can be T -dependent)⁴⁶,

$$\mu_{\text{eff}}(T) = \frac{\mu_{\text{eff}}(T_{\text{ref}})}{\chi_s^{\text{ref}}(T_{\text{ref}})} \chi_s(T), \quad (T > T_{\text{ref}}) \quad (28)$$

where T_{ref} is the reference temperature low or high enough to obtain the local moment (a matrix element with a T -dependent susceptibility⁴⁵), and $\chi_s^{\text{ref}}(T_{\text{ref}})$ and $\mu_{\text{eff}}(T_{\text{ref}})$ are the spin susceptibility and local moment (effective moment) at T_{ref} , respectively.

For $\text{Li}_{0.9}\text{Mo}_6\text{O}_{17}$ we choose $T_{\text{ref}} = 100$ K, the highest temperature at which the Curie-Weiss type paramagnetic susceptibility applies here [Eq. (20)] [note, above 100 K it is the Eq. (21) that describes the susceptibility]. Since $\chi_{\text{eff}}(T_{\text{ref}} = 100 \text{ K}) \approx 0.53 \times 10^{-4} \text{ cm}^3/\text{mol.FU}$, $\chi_{\text{eff}}(T = 300 \text{ K}) \approx 0.60 \times 10^{-4} \text{ cm}^3/\text{mol.FU}$, and from the Curie-Weiss constant $C \approx 7.8 \times 10^{-4} \text{ cm}^3 \cdot \text{K}/\text{mol.FU}$ (Section IV B) we have $\mu_{\text{eff}}(T_{\text{ref}} = 100 \text{ K}) = 2.82 \sqrt{C} \approx 0.08 \mu_B/\text{FU} = 0.08 \mu_B/(6 \text{ Mo ions}) \approx 0.013 \mu_B$ per Mo-ion, equation (28) gives $\mu_{\text{eff}}(T = 300 \text{ K}) \approx 0.015 \mu_B$ per Mo-ion, as a possible effective magnetic dipole moment of the Mo electrons.

This value μ_{eff} is ~ 100 times smaller than that of a spin $S = 1/2$ free electron, which has a magnetic dipole moment $\mu_{\text{free}} = \sqrt{4S(S+1)} \mu_B = 1.73 \mu_B$. The cause for this very small value of μ_{eff} for the Mo electrons in $\text{Li}_{0.9}\text{Mo}_6\text{O}_{17}$ is not clear¹⁷. On the other hand, any magnetic or non-magnetic impurities could also contribute to a local moment (especially at low temperatures)^{46,47}, but there has been no evidence to show that the low temperature Curie-Weiss susceptibility term [Eq. (20)] is from any magnetic or non-magnetic impurities, while there is no lattice imperfection here.

V. CONCLUSIONS

The magnetic dipole field at the atomic scale in a single crystal of quasi-one-dimensional (Q1D) paramagnetic conductor $\text{Li}_{0.9}\text{Mo}_6\text{O}_{17}$ is investigated both theoretically and experimentally, using a paramagnetic electron model and ^7Li -NMR spectroscopy measurements with an externally applied magnetic field $B_0 = 9$ T. The method is described in a general form and the field in the $\text{Li}_{0.9}\text{Mo}_6\text{O}_{17}$ is calculated as a function of the orientation angles (θ and ϕ) of B_0 in space, with experimental observations & demonstrations.

We find that the magnetic dipole field component $B_{||}^{\text{dip}}$ parallel to B_0 has no lattice axial symmetry; it is the smallest around the middle between the lattice a and c axes, with the central minimum to be 7.5° closer to the a than to the c axis in the ac -plane, while the maximum of $B_{||}^{\text{dip}}$ is 51.9° from the a -axis on the other side (in the same ac -plane), with a maximum value ~ 0.35 G when $B_0 = 9 \text{ T} \perp b$. The Mo ions could have a very small effective magnetic dipole moment μ_{eff} of $0.015 \mu_B$.

By minimizing potential magnetic contributions to the ^7Li -NMR spectrum satellites with the NMR spectroscopy measurements at the direction where the value of the magnetic dipole field is \sim the smallest ($\sim B_0 \parallel a$; $\theta = 90^\circ$ and $\phi = 0^\circ$), the behavior of the independent charge contributions is observed: there is no ^7Li -NMR spectrum satellite line broadening, i.e. no change in the charge distribution (including the value of EFG) from the Mo conduction electrons upon cooling over a wide range of temperatures.

Other related important physics quantities such as the spin susceptibility χ_s , DOS $D(E_F)$, and the Fermi energy E_F of the Mo electrons are also discussed.

This investigation demonstrates that the magnetic dipole field from the Mo electrons is the dominant source of the local magnetic fields at the Li site, and by the measurements of the ^7Li -NMR spectra at the direction where the value of the magnetic dipole field is \sim the smallest, we are able to observe the behavior of the charge contributions of the Mo conduction electrons directly at the atomic scale. This investigation suggests that the mysterious “metal-insulator” crossover at low temperatures is fundamentally not a charge effect. The work also reveals valuable local field information for further NMR investigation as recently suggested to be key important to the understanding of many mysterious properties of this Q1D material.

Acknowledgments

The work at University of West Florida was supported by SCA-2012 (G. Wu) and at UCLA by NSF Grant DMR-0334869 (WGC). We thank J. L. Musfeldt, J. R. Thompson, J. J. Neumeier, and S. E. Brown for helpful discussions.

-
- * Electronic address: gwu999@gmail.com (Guoqing Wu)
- ¹ P. Chudzinski, T. Jarlborg, and T. Giamarchi, *Luttinger liquid theory of purple bronze $\text{Li}_{0.9}\text{Mo}_6\text{O}_{17}$ in the charge regime*, Phys. Rev. B **86**, 075147 (2012).
 - ² T. Giamarchi, *Theoretical framework for the quasi-one dimensional systems*, Chem. Rev. **104**, 5037 (2004).
 - ³ J. Hager, R. Matzdorf, J. He, R. Jin, D. Mandrus, M. A. Cazalilla, and E. W. Plummer, *Non-Fermi-liquid behavior in quasi-one-dimensional $\text{Li}_{0.9}\text{Mo}_6\text{O}_{17}$* , Phys. Rev. Lett. **95**, 186402 (2005).
 - ⁴ M. Greenblatt, W. H. McCarroll, R. Neifeld, M. Croft, J. V. Waszczak, Solid State Commun. **51**, 671 (1984).
 - ⁵ W. H. McCarroll and M. Greenblatt, J. Solid State Chem. **54**, 282 (1984).
 - ⁶ O. Sepper and A. G. Lebed, Phys. Rev. B **90**, 094509 (2014).
 - ⁷ M. Nuss and M. Aichhom, Phys. Rev. B **89**, 045125 (2014).
 - ⁸ J. L. Cohn, S. Moshfeghyeganeh, C. A. M. dos Santos, and J. J. Neumeier, Phys. Rev. Lett. **112**, 186602 (2014).
 - ⁹ J. Dumas and C. Schlenker, Int. J. Mod. Phys. B **7**, 4045 (1993).
 - ¹⁰ J.-F. Mercure, A. F. Bangura, Xiaofeng Xu, N. Wakeham, A. Carrington, P. Walmsley, M. Greenblatt, and N. E. Hussey, Phys. Rev. Lett. **108**, 187003 (2012).
 - ¹¹ M. Greenblatt, Chem. Rev. **88**, 31 (1988).
 - ¹² M. Greenblatt, Int. J. Mod. Phys. B **7**, 3937 (1993).
 - ¹³ M. S. da Luz, J. J. Neumeier, C. A. M. dos Santos, B. D. White, H. J. Izario Filho, J. B. Leão, and Q. Huang, Phys. Rev. B **84**, 014108 (2011).
 - ¹⁴ C. A. M. dos Santos, B. D. White, Yi-Kuo Yu, J. J. Neumeier, and J. A. Souza, Phys. Rev. Lett. **98**, 266405 (2007).
 - ¹⁵ A. G. Lebed and O. Sepper, Phys. Rev. B **87**, 100511(R) (2013).
 - ¹⁶ M. Onoda, K. Toriumi, Y. Matsuda, and M. Sato, J. Solid State Chem. **66**, 163 (1987).
 - ¹⁷ J. Choi, J. L. Musfeldt, J. He, R. Jin, J. R. Thompson, D. Mandrus, X. N. Lin, V. A. Bondarenko, and J. W. Brill, Phys. Rev. B **69**, 085120 (2004).
 - ¹⁸ J.-F. Mercure, A. F. Bangura, Xiaofeng Xu, N. Wakeham, A. Carrington, P. Walmsley, M. Greenblatt, and N. E. Hussey, Supplemental Material at <http://link.aps.org/supplemental/10.1103/PhysRevLett.108.187003>.
 - ¹⁹ Y. Matsuda, M. Sato, M. Onoda, and K. Nakao, J. Phys. C: Solid State Phys. **19**, 6039 (1986).
 - ²⁰ X. Xu, A. F. Bangura, J. G. Analytis, J. D. Fletcher, M. M. J. French, N. Shannon, J. He, S. Zhang, D. Mandrus, R. Jin, and N. E. Hussey, Phys. Rev. Lett. **102**, 206602 (2009).
 - ²¹ M. S. da Luz, C. A. M. dos Santos, J. Moreno, B. D. White, and J. J. Neumeier, Phys. Rev. B **76**, 233105 (2007).
 - ²² C. Schlenker, H. Schwenk, C. Escribe-Filippini, and J. Marcus, Physica **135B**, 511 (1985).
 - ²³ N. Wakeham, A. F. Bangura, Xiaofeng Xu, F.-F. Mercure, M. Greenblatt, and N. E. Hussey, Nat. Commun. **2**, 396 (2011).
 - ²⁴ J. L. Cohn, B. D. White, C. A. M. dos Santos, and J. J. Neumeier, Phys. Rev. Lett. **108**, 056604 (2012).
 - ²⁵ J. Chakhalian, Z. Salman, J. Brewer, A. Froese, J. He, D. Mandrus, and R. Jin, Physica B **359** – **361**, 1333 (2005).
 - ²⁶ J. D. Denlinger, G.-H. Gweon, J. W. Allen, C. G. Olson, J. Marcus, C. Schlenker, and L.-S. Hsu, Phys. Rev. Lett. **82**, 2540 (1999).
 - ²⁷ J. Merino and R. H. McKenzie, Phys. Rev. **85**, 235128 (2012).
 - ²⁸ C. P. Slichter, *Principles of Magnetic Resonance* (Springer, Berlin, 1989), 3rd ed..
 - ²⁹ A. Abragam, *The Principles of Nuclear Magnetism* (Clarendon, Oxford, 1962).
 - ³⁰ G. C. Carter, L. H. Bennett, and D. J. Kahan *Metallic Shifts in NMR*(Pergamon, London, 1977), part I. Guoqing Wu *et al.*, Phys. Rev. B **74**, 064428 (2006).
 - ³¹ W. C. Dickinson, Phys. Rev. **81**, 717, (1951).
 - ³² L. E. Drain, Proc. Phys. Soc. London **80**, 1380 (1962).
 - ³³ R. Dickinson, A. T. Royappa, F. Tone, L. Ujj, and Guoqing Wu, J. Appl. Phys. **110**, 013902, (2011).
 - ³⁴ J. D. Jackson, *Classical Electrodynamics* 2nd ed. (Wiley, Singapore, 1990).
 - ³⁵ N. W. Ashcroft and N. D. Mermin, *Solid State Physics*, 1st ed. (Holt, Rinehart and Winston, New York, 1976).
 - ³⁶ G. B. Arfken and H. J. Weber, *Mathematical Methods for Physicists*, 4th ed. (Academic Press, Inc., San Diego).
 - ³⁷ J. J. Neumeier, private communication.
 - ³⁸ Guoqing Wu *et al.*, *NMR Investigation of Quasi – One – Dimensional Conductor $\text{Li}_{0.9}\text{Mo}_6\text{O}_{17}$* , to be published.
 - ³⁹ Z. S. Popović, and S. Satpathy, Phys. Rev. B **74**, 045117 (2006).
 - ⁴⁰ C. A. M. dos Santos, J. Moreno, B. D. White, and J. J. Neumeier, Phys. Rev. B **76**, 233105 (2007).
 - ⁴¹ N. W. Ashcroft and N. D. Mermin, *Solid State Physics*, 1st ed. (Holt, Rinehart and Winston, New York, 1976).
 - ⁴² J. L. Musfeldt and J. R. Thompson, private communication.
 - ⁴³ M. Acharyya, Commun. Theor. Phys. **55**, 901 (2011).
 - ⁴⁴ A. M. Clogston, B. T. Matthias, M. Peter, H. J. Williams, E. Corenzwit, and R. C. Sherwood, Phys. Rev. **125**, 541 (1962).
 - ⁴⁵ V. Grinenko, K. Kikoin, S.-L. Drechsler, G. Fuchs, K. Nenkov, S. Wurmehl, F. Hammerath, G. Lang, H.-J. Grafe, B. Holzapfel, J. van den Brink, B. Bchner, and L. Schultz, Phys. Rev. B **84**, 134516 (2011).
 - ⁴⁶ H. Alloul, J. Bobroff, M. Gabay, and P. J. Hirschfeld, Rev. Mod. Phys. **81**, 45 (2009).